Contrasting biophysical controls on carbon dioxide and methane outgassing from streams

L. Rovelli[1,*], L. A. Olde[2,‡], C. M. Heppell[3], A. Binley[4], G. Yvon-Durocher[5], R. N. Glud[6,7,8] and M. Trimmer[2,*]

[1] iES - Institute for Environmental Sciences, University of Koblenz-Landau, 76829 Landau, Germany.

[2] School of Biological & Chemical Sciences, Queen Mary University of London, London E1 4NS, United Kingdom.

[3] School of Geography, Queen Mary University of London, London E1 4NS, United Kingdom.

[4] Lancaster Environment Centre, Lancaster University, Lancaster, LA1 4YQ, United Kingdom.

[5] Environment and Sustainability Institute, University of Exeter, Penryn, Cornwall, TR10 9EZ, United Kingdom.

[6] HADAL & Nordcee, University of Southern Denmark, 5230 Odense M, Denmark.

[7] Danish Institute of Advanced Study – DIAS, University of Southern Denmark, 5230 Odense M, Denmark.

[8] Department of Ocean and Environmental Sciences, Tokyo University of Marine Science and Technology, 108-8477 Tokyo, Japan.

[*] Corresponding authors: Mark Trimmer (m.trimmer@qmul.ac.uk) and Lorenzo Rovelli (rovelli@uni-landau.de)

[‡] now at Rothamsted Research, West Common, Harpenden, AL5 2JQ, United Kingdom.

Key Points:

- There are different controls on the outgassing of the greenhouse gases carbon dioxide and methane in streams.
- Carbon dioxide results largely from physical run-off from the land and is then altered in stream by biology depending on season.
- In contrast, methane is created in the streambed but once released to the stream is then dissipated by the physical forces of stream flow.

Abstract

Small headwater streams are recognized for intense outgassing to the atmosphere of climate-relevant carbon dioxide (CO_2) and methane (CH_4). Though these headwaters are markedly oversaturated for both CO_2 and CH_4, the origins and controls over the fate of these two carbon-gases are still poorly constrained, especially for the stronger greenhouse gas CH_4. Here, by measuring stream-based production of CO_2 and CH_4, concurrently with their rates of outgassing to the atmosphere, we identify distinct biophysical control mechanisms for each gas. We show that while CO_2 is largely imported from the catchment in proportion to discharge, CO_2 outgassing can be modulated by in-stream metabolism to offset outgassing by up to 30% in spring and summer. In contrast, CH_4 shows a non-linear response to seasonal changes in discharge and is predominantly produced in the streambed in relation to sediment type. Further, once released from the streambed, outgassing of CH_4 at the surface and flow-driven dilution occur far more rapidly than biological methane oxidation and CH_4 leaves the water largely unaltered by biology. Incorporating the intense carbon cycling of headwater streams into the global carbon cycle will require distinct parameterizations for each carbon gas in Earth system models.

Plain Language Summary

There is growing interest in the global carbon cycle and how carbon is transformed in the landscape into the greenhouse gases carbon dioxide (CO_2) and methane – with methane being by far the more potent than CO_2. Streams and rivers are recognized hotspots of carbon cycling in the landscape, commonly harboring large amounts of CO_2 and methane – yet what controls either gas in streams is not fully understood. Without that understanding, we cannot predict how carbon cycling will respond to climate change or to other human alteration of the landscape. Here we researched different components of the carbon cycle in streams to show that each gas is influenced by quite distinct "biophysical" control mechanisms. While CO_2 in streams results largely from physical run-off from the land, once in a stream it can be changed by the stream biology that ebbs and flows with the seasons. Contrastingly, methane is largely created by biology within the streambed itself but once released into the wider stream that methane is then dissipated by the physical forces of stream flow. Put more

simply, CO_2 is physically carried to the stream to then be altered by biology, whereas as methane is borne from biology in the stream, to then be physically carried away.

1 Introduction

Rivers and streams transport, store and transform large quantities of carbon (Battin et al., 2009; Cole et al., 2007) and are routinely supersaturated with the two climatically important carbon gases methane (CH_4) and carbon dioxide (CO_2) which they outgas to the atmosphere (Raymond et al., 2013; Stanley et al., 2016). Small headwater streams (<20 km^2 catchment area) consistently have the highest oversaturation for CO_2 and, despite their small extent, contribute some 36% (i.e., 0.93 Pg C yr^{-1}) of the total CO_2 outgassing from river networks globally (Marx et al., 2017). In contrast, headwater streams appear no more saturated in CH_4 than larger rivers and estimated CH_4 outgassing rates are similar across streams and rivers of comparable sizes (Stanley et al., 2016). Hence, the origins and fate of these two important carbon gases in headwater streams appear different. While we understand more about CO_2 compared to CH_4 in rivers and streams (Stanley et al., 2016) in general, the origins and final fates of both carbon gases remain poorly constrained (Crawford & Stanley, 2016; Striegl et al., 2012).

The supersaturation and subsequent outgassing of CO_2 and CH_4 throughout river networks can be due to both carbon metabolism in the bed and gases imported from the catchment (Butman & Raymond, 2011; Crawford & Stanley, 2016; Jones & Mulholland, 1998b; Peter et al., 2014; Sanders et al., 2007; Striegl et al., 2012), including weathering for CO_2. For CO_2, terrestrial inputs can be the dominant source of CO_2 emitted from the river (Butman & Raymond, 2011; Striegl et al., 2012), though the magnitude of this component is dependent on river and stream size and seasonal changes in discharge (Hotchkiss et al., 2015). Before CO_2 is finally outgassed, there can be further modulation by net ecosystem production depending on season and diel cycle (Lynch et al., 2010; Peter et al., 2014; Reiman & Xu, 2018; Rocher-Ros et al., 2020; Stets et al., 2017), but these biological dynamics have not been quantified directly and remain essentially unknown for CH_4.

Despite the relative paucity of data for CH_4 in rivers and streams, their estimated total annual outgassing has recently been revised upwards from 1.5 Tg CH_4 yr^{-1} in 2011 (see Bastviken et al., 2011), to 26.8 Tg CH_4 yr^{-1} in 2016 (Stanley et al., 2016) and 30.3 Tg CH_4 yr^{-1} in 2021(Li et al., 2021) which highlights the growing evidence for the significance of running waters in the global CH_4 budget. For example, the recent revision increases the total contribution from rivers, streams and lakes to global CH_4 emissions from 40 Tg CH_4 yr^{-1}, to 70.3 Tg CH_4 yr^{-1}, which is equivalent to 32% of that emitted from wetlands (217 Tg CH_4 yr^{-1};

Ciais et al., 2013). As CH_4 is a far more potent greenhouse gas than CO_2 (Myhre et al., 2013), the partitioning between either carbon gas emitted from rivers and streams is particularly relevant to climate forecasting. In addition, anthropogenic land use change and habitat destruction are likely to have a relatively greater influence on riverine CH_4 dynamics (Crawford & Stanley, 2016; Sanders et al., 2007; Yu et al., 2017), compared to CO_2. Despite these concerns, our understanding of the contemporaneous biophysical controls of these two carbon gases in rivers and streams in general is still lacking (Jones & Mulholland, 1998b; Yu et al., 2017).

The aim of this study was to characterize how discharge and in-stream carbon metabolism together exert biophysical controls on the sources and final fates of CO_2 and CH_4 in temperate, low-gradient headwater streams (maximum catchment area of ~60 km^2) in our case study catchment of the lowland Hampshire River Avon, UK. Within the catchment, we performed a seasonal study on six streams with distinct geologies (two each on the clay, Greensand and Chalk) and over a wide spectrum of hydrological characteristics, e.g., flashy to stable hydrograph, hydrological connectivity to the land and in-stream carbon metabolism (see Heppell et al., 2017; Rovelli et al., 2017, 2018). To quantify how much outgassing of CO_2 and CH_4 could be accounted for by either in-stream production or input from the catchment, we combined: i) traditional measurements of benthic metabolism via isolated benthic chambers (Trimmer et al., 2009) with; ii) integrated estimates of whole stream metabolism using the state-of-the-art and non-invasive aquatic eddy covariance technique (Rovelli et al., 2017, 2018); and iii) direct quantification of CO_2 and CH_4 outgassing from anchored floating chambers (Podgrajsek et al., 2014) (see Figure 1). The seasonal study was complemented by measurements of CO_2 and CH_4 concentrations in riparian soils and streambeds and laboratory-based assessments of the potential for methane oxidation in the water column. Finally, we made high-temporal-resolution day and night measurements of CO_2 and CH_4 outgassing and modeled any diel changes as functions of our directly parameterized biological (e.g., net ecosystem metabolism, water column methane oxidation) and physical control mechanisms (e.g., dilution, reaeration, outgassing).

2 Materials and Methods

2.1 Study site

This study was performed in six ~150 m headwater reaches of the lowland catchment of the Hampshire River Avon (UK) (Figure 1a; Allen et al., 2014; Jarvie et al., 2005). The headwaters drain three dominant geologies: Chalk (River Ebble and River Wylye), (Upper) Greensand, i.e., fine-grained glauconitic sands and sandstones, (River Nadder and West Avon) and clay (River Sem and Priors), although some sub-catchments and reaches encompass a combination of those geologies, e.g., clay and Greensand on River Nadder, Chalk and Greensand on River Wylye (Figure 1a). Here, we regard these sub-catchments based on their dominant underlying geology, which has been shown to modulate the local hydrology and hydrological connectivity (Bristow et al., 1999). Parallel studies at these reaches have also directly linked hydrological regime and baseflow index (BFI) to the dynamics of key stream sediment processes such as nitrogen gas (N_2) production (Lansdown et al., 2016), and nutrient dynamics (Heppell et al., 2017). Integrated baseflow, as a proportion of total flow over a single day, has also been identified as a robust predictor of seasonal differences in stream metabolism dynamics across the different reaches (Rovelli et al., 2017). The water column of these lowland headwaters has been shown to contribute to about a quarter of their annual whole-stream respiration and primary production, with water column respiration in the turbid waters, e.g. River Sem on the clay, contributing, on average, 71.3% of the spring and summer whole-stream respiration (Rovelli et al., 2017, 2018). Surface water sampling by Heppell et al. (2016a) has shown that mean pH remained largely comparable across the sites ranging from 7.3 to 7.7, although with the clay streams tending towards lower values. In contrast, mean dissolved inorganic carbon (DIC) was, on average, highest in the Chalk streams and in the Greensand West Avon (3.9 to 4.8 mmol L^{-1}) and lowest in Greensand Nadder and in the clay streams (3.0 to 3.1 mmol L^{-1}). Estimates of total alkalinity based on pH and DIC (after Millero, 1979) were in the order of 2650 to 2900 µmol L^{-1} (clay streams and Nadder) and 3600 to 4520 µmol L^{-1} (chalk streams and West Avon), respectively.

For the purposes of this study, each reach was studied for a period of one to three days in spring, summer, autumn and winter from April, 2013, until February, 2014. Using a variety of techniques (Figure 1), we quantified fluxes of dissolved oxygen (O_2), carbon dioxide (CO_2) and methane (CH_4) using chambers (benthic and floating) and O_2 fluxes via aquatic

eddy covariance (Rovelli et al., 2017, 2018), along with stream morphological characteristics and local hydrological regime (Heppell et al., 2017). We experienced from below average rainfall in both spring and summer, to a 100-year flood in the winter of 2013 to 2014 and while this allowed us to capture a wide range of stream discharges it was not possible to sample during the extreme flood (see Figures S1, S2). We used piezometers to measure porewater concentrations of CH_4 and CO_2 in riparian soils and streambed sediments every two months (Heppell et al., 2017). A high-resolution survey of day and night CO_2 and CH_4 outgassing was performed in spring, 2015, using an automated floating gas chamber connected to an Ultraportable Greenhouse Gas Analyzer (UGGA; Los Gatos Research, California, USA). Benthic mapping surveys were also performed in each reach for each season to characterize the areal coverage of vegetated and non-vegetated patches of clay, Greensand and Chalk gravel following the methods described in Gurnell et al. (1996). The patch type areas were drawn manually onto local geo-referenced stream maps, and were digitized using Adobe Photoshop® to extract relative areal coverage (in percentage) of each sediment patch-type.

2.2 Benthic metabolism and sediment CH_4 release.

Measurements of *in situ* O_2-based benthic metabolism, along with release of CH_4, were performed at the patch scale (<1 m^2) using benthic chambers (Figure 1b; Trimmer et al., 2009). These consisted of transparent Perspex chambers (0.5 L enclosed volume, 73 cm^2 surface area) mounted on a steel-ring, which were used to measure net benthic O_2 production and CH_4 release in the light (n = 12, daytime), and equally-sized black, plastic chambers to measure benthic O_2 consumption and CH_4 release in the dark (n = 12, night-time). Potassium chloride was added as a tracer to quantify potential exchange of water from the chamber in the permeable sand and gravel-Chalk beds. The chamber incubations covered the range of sediment patch types identified during the initial stream habitat mapping. Each chamber deployment lasted ~2 hours, and four chambers were deployed each day/night over three successive days. The chambers were continuously stirred using a magnetic stirrer. Changes in O_2 concentration within the benthic chamber were monitored at one-minute intervals using Clark-type oxygen microelectrodes connected to an Under-Water Meter (Unisense, Denmark) (Trimmer et al., 2010). Water samples for CH_4 analysis were taken from the chamber at the

beginning and end of each deployment using a syringe connected to a valve on top of the chambers (Figure 1b).

Samples for CH_4 were transferred gently to 12mL gas-tight vials (Exetainers, Labco, UK), overfilled to ensure no air was introduced, and preserved within two hours of being taken by adding 100µl zinc chloride solution (7M; see Dalsgaard et al., 2000). CH_4 was measured after headspace equilibration using a gas chromatograph fitted with a flame ionization detector (Agilent Technologies, UK) and concentrations calculated using solubility coefficients (Yamamoto et al., 1976) following established protocols (e.g., Sanders et al., 2007). Rates of O_2 consumption or production over time were calculated using linear-regression and scaled to an areal flux (in mmol m^{-2} h^{-1}) using the chamber inner dimensions. Similarly, CH_4 consumption or production rates were calculated using the concentration at the start and end of each deployment. Final rates of benthic gas exchange were scaled-up to the reach using our benthic mapping of each sediment patch type (vegetated, clay, Greensand and Chalk gravel), by weighting the respective patch-averaged rates by the relative areal coverage (in percentage) of each sediment patch-type within the reach. Benthic O_2 exchange was used to estimate reach-scale benthic ecosystem respiration (ER, as mmol CO_2 produced per m^{-2} h^{-1}), benthic gross primary production (GPP, as mmol CO_2 consumed per m^{-2} h^{-1}) and net benthic ecosystem metabolism (in mmol CO_2 m^{-2} h^{-1}) assuming a 1 to 1 ratio for O_2 to CO_2 (Glud, 2008). It is well established that this ratio may vary over the diel cycle, across seasons as well as spatially, within a commonly reported rage of 0.8 to 1.2 (e.g., Glud, 2008; Therkildsen & Lomstein, 1993). As changes in the ratio will proportionally affect our rates, these are to be considered conservative estimates. Throughout the manuscript, positive CO_2 net benthic metabolism will be used to indicate a release of CO_2 from the benthic compartment into the water column, i.e., a net source of CO_2. The mean benthic gas exchange from each sediment patch type across all sites was estimated by data clustering following a signed logarithmic transform (see Section 2.7).

2.3 Seasonal outgassing of CO_2 and CH_4.

Outgassing of CO_2 and CH_4 was quantified using anchored floating chambers (8.6 L volume and 674 cm^2 surface area; Figure 1c) which were deployed in parallel to the benthic chambers (Podgrajsek et al., 2014). The floating chambers consisted of an inverted plastic bowl covered in reflective aluminum tape, fitted with a polyurethane tubing sample port to allow for gas-sampling via a three-way luer-lock valve and a CO_2 sensor (SenseAir; Delsbo,

Sweden) (Bastviken et al., 2015). Typical chamber deployments lasted two hours and were performed in the morning, with the CO_2 sensor set to measure at 5-minute intervals. For CH_4, discrete gas samples were taken at regular intervals from the sample port using a gas-tight syringe (SGE International Pty Ltd, Australia) and stored for later analysis by displacing de-gassed, de-ionised water from 3mL gas-tight vials (Exetainers, Labco, UK). Gas samples were analyzed by GC-FID for CH_4 as described above. For each chamber deployment the initial period of linear rise in gas was identified and the change in concentration over this period was converted into outgassing rates using linear regression and the chamber's dimensions. Positive outgassing rates indicate an upward exchange from the streams into the atmosphere, i.e., a net atmospheric source, while negative rates indicate a downward exchange from the atmosphere into the stream system, i.e., a net atmospheric sink. It should be also noted that anchored floating chambers, compared to freely-drifting chambers, might enhance near-surface turbulence and thus bias outgassing rates (Lorke et al., 2015). Although such bias can be substantial in fast flowing, high-gradient streams, flows in our low-gradient streams (Rovelli et al., 2017, 2018) fell below this threshold (see Lorke et al., 2015).

2.4 High-temporal-resolution diel measurements of CO_2 and CH_4 outgassing (spring 2015).

The seasonal outgassing measurements were complemented by an intensive campaign in spring 2015, to characterize short-term outgassing dynamics in each stream. A LiCor Long-Term Chamber (Model 8100-101; LiCor, Nebraska, USA, with a volume of 4.093 L and a surface area of 318 cm^2) was modified to float on the streams by mounting it on a plastic cylinder (collar) and life-ring (Figure 1c) and with a total volume (chamber + collar) of 6.29 L. The chamber was connected to a CR800-Series Datalogger (Cambell Scientific Inc, Utah, USA) to control the motorized chamber. During the deployment, the chamber was set to alternately open and close every 10 minutes to flush the chamber and prevent it from equilibrating with the underlying water. Concentrations of CO_2, CH_4 and water vapor were measured at 10 second intervals with an Ultraportable Greenhouse Gas Analyzer (Los Gatos Research, California, USA), attached to the chamber by a closed-loop (Figure 1d). Gas fluxes, corrected for water vapor dilution, that accounted for the opening and closing of the chamber, were computed for each of the consecutive 10 minute closed-chamber intervals using self-written R (R Core Team, 2014) and Matlab® scripts. An r^2 value of 0.9 was used as quality cut-off to flag weak regressions.

We also characterized methane ebullition events by analyzing the distribution of the rates of change in CH_4 (in ppm s^{-1}) during all 1416 measurements. Here we ascribed any sharp episodic increase in CH_4 concentration (i.e., sharp peaks increases, see Figure S9) that lasted for at least two or more consecutive data points to an ebullition event and delineated those from steady, diffusional increases in CH_4 (Figure S9). We found that a 5-fold peak increase in the rate of change over the diffusional rate of increase, was the optimal threshold to identify ebullition events. Once identified, these events were subsequently cross-checked against the parallel CO_2 readings to discriminate between ebullition and other non-steady state fluxes or deployment issues (e.g., inadequate sealing, suboptimal flushing of the chamber), which would also result in clear deviation from a linear change in CO_2. The significance of ebullition was quantified in terms of numbers of ebullition events, as well as the overall contribution from ebullition to CH_4 outgassing (single measurements and mean). The latter was estimated as the total rate of CH_4 outgassing (diffusion + ebullition), by computing a point-to-point slope from the first point at the beginning of the (diffusive) linear slope, before an ebullition event, and the last point of the linear slope after an ebullition event (see Figure S9).

2.5 Whole stream carbon metabolism.

An integrative assessment of whole-stream benthic metabolism in each stream was obtained seasonally using the non-invasive aquatic eddy covariance technique (Berg et al., 2003). Aquatic eddy covariance measurements in rivers and streams quantify the dynamics and driving forces of benthic stream metabolism and riverine O_2 gas exchange (Berg et al., 2003; Berg & Pace, 2017; Koopmans & Berg, 2015; Murniati et al., 2015; Rovelli et al., 2017, 2018). In essence, the technique relies on the simultaneous acquisition of high-resolution time series (64 Hz) of both vertical flow velocity and dissolved O_2 concentrations at the same point in the water above the sediment from which turbulence-driven fluctuations in both vertical velocity and O_2 can be extracted. With the appropriate setup and procedures (see Berg et al., 2003; Lorrai et al., 2010; Rovelli et al., 2017, 2018), the co-variance of those fluctuations provides instantaneous O_2 flux estimates that are then averaged over time (e.g., hours or days) to provide a net estimate of O_2 uptake or release from the sediment. Model validations of the aquatic eddy covariance have shown that the obtained O_2 flux integrates contributions from a theoretically constrained area of the sediment, termed the footprint area,

whose extent depends on: i) the distance from the sediment in which the measurements are collected; and ii) specific characteristics of the sediment surface roughness (i.e., bottom roughness length scale) (see Berg et al., 2007). The aquatic eddy covariance technique may capture benthic O_2 fluxes over much larger areas of the streambed (tens of m^2 footprint) and was, therefore, complimentary to the patch-scale measurements made with the benthic chambers (described above).

Our aquatic eddy covariance system consisted of an acoustic Doppler velocimeter (Vector, Nortek A/S, Rud, Norway), Clark-type O_2 microelectrodes (Revsbech, 1989) and submersible amplifiers (McGinnis et al., 2011) and was operated as described in McGinnis et al. (2016) (Figure 1e). Aquatic eddy covariance was used to quantify benthic GPP, ER and net benthic metabolism, while light and dark incubations of discrete water samples (Rovelli et al., 2017, 2018) captured the same parameters in the water to enable us to quantify net, whole stream metabolism (NWM) within each stream reach. This includes contributions from the sediments, water column and aquatic plants to integrate in-stream metabolism at the reach scale (20 to 70 m^2). Measurements were made over at least two and half of the three day sampling period at each site. A comprehensive description of the seasonal aquatic eddy covariance work performed within River Sem, River Nadder and River Wylye, as well as Ebble and West Avon in spring, is presented elsewhere (Rovelli et al., 2017, 2018, 2016). Within the remit of this study, we only report the O_2-based net whole-stream metabolism (in mmol m^{-2} h^{-1} or mmol m^{-2} d^{-1}) as CO_2, assuming a 1 to 1 ratio of O_2 to CO_2 for metabolic activity (see section 2.2.). As for the benthic chambers, positive net whole-stream metabolism indicates a net release of CO_2 from the benthic compartment into the water column, while negative values indicate a net benthic uptake of CO_2.

2.6 Water column oxidation and dilution of streambed CH_4.

Estimates of water column methane oxidation rate potentials were obtained for each stream from laboratory-based measurements of methane oxidation rate potentials of suspended particulate matter (SPM, in mg L^{-1}), scaled to *in situ* suspended particulate matter and CH_4 concentrations, following Shelley et al. (2014, 2015). For each site, methane oxidation was measured at a standard CH_4 concentration of 8 µmol L^{-1} with 100%, 62.5%, 37.5% and 0% of the original suspended particulate matter concentration. Gas samples were taken from the headspace at five time points over the incubation period (0 h, 26.5 h, 49 h, 122.5 h, and 168 h, respectively) and measured as above and an empirical relationship

between suspended particulate matter and methane oxidation derived (Figure S4). Rates of methane oxidation (in nmol CH_4 g^{-1} SPM h^{-1}) were obtained via linear regression and subsequently scaled from the standard laboratory concentration (C_{stand} = 8 µmol CH_4 L^{-1}) to *in situ* CH_4 concentrations ($C_{in\ situ}$) using our previously, laboratory established empirical Michaelis–Menten kinetic relationship between methane oxidation rate (MO) and CH_4 concentration (~0.01 to 22 µmol L^{-1}) for fine sediment (Shelley et al., 2015):

$$MO(C_{in\ situ}) = V_{max} C_{in\ situ} / (K_m + C_{in\ situ}) \qquad \text{equation (1)}$$

with the maximum rate (V_{max}) equal to 586 nmol CH_4 g^{-1} h^{-1} and the Michaelis constant (K_m) being 3.7 µmol L^{-1} for C_{stand} between ~0.01 to 22 µmol CH_4 L^{-1}. Background CH_4 concentrations for each stream were obtained from the initial measurements at the beginning of each benthic chamber incubation (t_0). The potential for methane oxidation associated with stream-water suspended particulate matter to alter CH_4 concentrations in the water column was calculated using the methane oxidation rates and the *in situ* ratio of CH_4 concentration to suspended particulate matter for each stream. The resulting parameter, here termed, Rk_{CH4} (in h^{-1}) represents a measure of the turnover time for CH_4 in the water column due to biological activity. The residence time of CH_4 due to outgassing, here quantified as the reaeration constant for K_{CH4} (in h^{-1}), was obtained from standardized gas transfer velocities (k_{600}, in m d^{-1}) estimated for each stream using hydraulic equations (see Section 2.7), accounting for mean water depths and the Schmidt number for CH_4 at *in situ* stream temperatures (Raymond et al., 2012). Flow driven dilution of CH_4, here termed K_{flow}, was defined as the residence time of water (in h^{-1}) within any stream reach driven by local discharge. A comparison of the ratios between these parameters enables an assessment of their relative importance in modulating water column CH_4 dynamics. For instance, a ratio of Rk_{CH4} to K_{CH4} or K_{flow} close to 1 would indicate that microbial, methane oxidation is a major driver of changes in water column CH_4 concentrations.

2.7 Mass-balance of diel CO_2 and CH_4 dynamics.

The obtained fluxes and field measurements were combined into a simple mass-balance model to further investigate potential controls on diel changes in dissolved CO_2 and CH_4 concentration dynamics at the reach scale. Here, concentration changes of CO_2 and CH_4 over time (dC/dt, in mmol m^{-3} h^{-1}) were modeled based on: (i) the amount of dissolved gas coming into the reach from upstream, including from the catchment (F_{in}); (ii) the net gas release or uptake across the entire streambed surface area of the reach ($F_{streambed}$); (iii) net

biology-mediated gas production or consumption within the water column as it moves through the reach ($F_{\text{water column}}$); (iv) the net amount of outgassing to the atmosphere occurring across the entire water surface area of the reach ($F_{\text{outgassing}}$); and (v) the amount of dissolved gas being discharged downstream at the lower end of the reach (F_{out}) as:

$$\frac{dC}{dt} = F_{in} + F_{streambed} + F_{water\ column} - \frac{A}{V}F_{outgassing} - F_{out} \qquad \text{equation (2)}$$

In Equation 2, F_{in} (in mmol m^{-3} h^{-1}) is quantified as the dissolved gas concentration upstream of the reach ($C_{\text{upstream,}}$ in mmol m^{-3}) multiplied by water discharge (m^3 h^{-1}) at the upper end of the reach, which were both assumed constant throughout the model run. Similarly, F_{out} (in mmol m^{-3} h^{-1}) was computed at each time step as the final modeled stream concentration from equation 2, for the previous time step, multiplied by the discharge out of the reach, starting from $C_{\text{background}}$ (t = 0, in mmol m^{-3}). The model was run for up to 6 h with time steps of 5 s and a control volume (V) of mean stream width x 150 m length (along the flow direction) x mean stream depth (in m), assuming a constant stage (i.e., water level). The model focuses on the difference in CO_2 and CH_4 dynamics between day and night and we assume a constant rate of supply or loss of these gases from each pathway over the model run. The modeled mass balance does not include lateral and vertical groundwater recharge and discharge, respectively, which we know to be comparatively minor on the modeled time scales (e.g., Rovelli et al., 2018). Water column gas concentrations in the reach come from field measurements during summer, 2013, and were used for both the initial (t = 0) concentration within the reach ($C_{\text{background}}$, in mmol m^{-3}) and C_{upstream}. For CO_2, $F_{\text{streambed}}$ (in mmol m^{-3} h^{-1}) is the day and night aquatic eddy covariance O_2-flux (in mmol m^{-2} h^{-1}) multiplied by the area-to-volume (A/V) ratio of the control volume, while $F_{\text{water column}}$ (in mmol m^{-3} h^{-1}) is the O_2-flux in bottle incubations with both expressed as CO_2 equivalents using a 1 to 1 molar ratio as above (Rovelli et al., 2017). These were chosen over invasive chamber-based fluxes as they are, overall, expected to provide more accurate estimates of daytime primary production, and more constrained benthic uptake rates in permeable sediments (e.g., Attard et al., 2015). For CH_4, $F_{\text{streambed}}$ is the measured sediment CH_4 release, obtained from the light or dark benthic chambers (in mmol m^{-2} h^{-1}) multiplied by A/V, while the suspended particulate matter-scaled methane oxidation rates, in mmol m^{-3} h^{-1}, were used for $F_{\text{water column}}$. Positive values of $F_{\text{water column}}$ and $F_{\text{streambed}}$ indicate a source of CO_2 and CH_4 within the water column or a net gas exchange from the benthic compartment into the water

column, respectively. Reach-scale outgassing (in mmol m^{-2} h^{-1}) for both CO_2 and CH_4 was quantified as:

$$F_{outgassing} = -[k(C_{sat} - C)] \quad \text{equation (3)}$$

from gas concentrations in the streams (C) and equilibrial atmospheric concentrations (C_{sat}) (Weiss, 1974; Wiesenburg & Guinasso, 1979), with positive values indicating a net atmospheric source, i.e., a net gas exchange from the stream into the atmosphere. Gas transfer velocities (k, m h^{-1}) were obtained from k_{600} values scaled by the respective Schmidt numbers for each gas at in situ water temperature (Raymond et al., 2012). Values of k_{600} were quantified from stream discharge and site-specific hydraulic parameters, based on the average output from the seven model parametrizations provided by Raymond et al. (2012), which were validated previously for two of the investigated streams (see Rovelli et al., 2018). Temperature time series were obtained from Heppell & Parker (2018).

The model requires meaningful estimates of the average day and night benthic CH_4 fluxes for the dominant streambed patches e.g., vegetated and non-vegetated sand and Chalk gravel, as well as for clay. Due to the limited amount of data and the inherent heterogeneity of benthic CH_4 flux measurements, values tended to span several orders of magnitude and were often characterized by a strong skewness towards higher values (Fig. 2). To minimize the risk of biasing our mean estimates, the data were transformed as $y = sign(x) \times ln(|x| + 1)$ to ensure that the original sign of the flux would be maintained. The transformed data were then averaged into clusters in full digit increments (e.g., -1 to 0, 0 to 1, …) to give each cluster equal weighting. The resulting monotonic dataset was subsequently averaged, and the obtained averaged value ($ln\_average$) converted back a mean flux as $F_{mean} \approx sign(\ln\_average) \times e^{|ln\_average|}$. Note that the flux dataset for the gravel patch type were found to be more constrained than for the other patch types, with 75% of the data falling within the -0.9 to 1.3 µmol m^{-2} h^{-1} range, and the outliers deviating by a factor of 3 to more than 600. Given the reduced magnitude of the flux range, the data were averaged arithmetically.

The model was first used to reproduce the CO_2 dynamics, matching the observed daytime outgassing by fine-tuning both the stream discharge and background CO_2 and CH_4 concentrations to within the range provided by the field observations, e.g., mean, median for the month (Heppell & Binley, 2016a, 2016b; Rovelli et al., 2017). Model performance was

evaluated by comparing the resulting modeled night-time outgassing rates, with the mean values obtained during our high-resolution sampling campaign. The same hydrological parameters, once validated for CO_2, were then applied to CH_4, where the fine-tuning of the model was only performed on the background concentrations. The model was also used to investigate the relevance of different physical and biology-mediated parameters in driving diel changes in CO_2 and CH_4 outgassing, via a measurements-oriented sensitivity analysis. This included discharge dynamics and diel temperature changes (Heppell & Parker, 2018) that were evaluated for both gases, as well as gas specific parameters, such as the respiratory quotient to covert O_2 fluxes to CO_2 equivalents and suspended particulate matter concentrations (Heppell & Binley, 2016b), used as a descriptor for methane oxidation in the water column. While *k* is parametrized in the model as described above, and thus coupled to stream discharge, *k* values associated the lower and upper end of the observed discharge were also applied to the base model to assess the sensitivity of the diel outgassing dynamics to changes in gas transfer velocity.

2.8 Statistical Analysis.

We used linear mixed effects models with the lme4 package in R (Bates et al., 2015; Pinheiro & Bates, 2000; R Core Team, 2014) to estimate the overall main effect of light, season, patch type (gravel, sand, clay and vegetated sediment) or individual stream on measured benthic O_2 and CH_4 exchange. For example, to isolate the overall main effect of light we pooled the data for each stream and each seasonal campaign and fitted models that included season and stream as random effects on the intercepts (see Tables S1 to S3). Note, that the effect of patch type was not tested in the turbid clay streams as the beds were homogenous, i.e., there were no vegetated patches. Similarly, we modeled the overall main relationship between outgassing and discharge for CO_2 or CH_4 by pooling the data from each seasonal campaign and fitting slopes and intercepts as random effects to the data for each stream. In each case, nested models of varying complexity, e.g., models with random slopes and intercepts *versus* random intercepts only, were compared using the Akaike Information Criterion (AICc for small samples sizes) with the "MuMin" package (Barton, 2009) and final parameter estimates for the most parsimonious models derived using the "emmeans" package (Lenth, 2019). Where appropriate, the overall relationship in the data is visualized by plotting the partial residuals from the mixed-effects model. Data with a high degree of skewness were

cube-root ($\sqrt[3]{}$) transformed to improve normality and to maintain the original positive and negative value structure in the data (Miles et al., 2013; Zuur et al., 2009). Further details are given in the Supplementary Information.

3 Results

3.1 Seasonal field campaigns

3.1.1 CO_2 fluxes, outgassing *versus* discharge and porewater concentrations

Rates of CO_2 outgassing (in mmol m^{-2} h^{-1}) from the streams, quantified with floating chambers, were strongly seasonal, ranging from 3.95 ± 0.63 (4.12) (mean ± standard error (median)) in spring, to 16.66 ± 2.67 (13.07) during winter (Figure 2a), while chamber-based net benthic metabolism (in mmol m^{-2} h^{-1}) ranged from -0.10 ± 0.51 (-0.34) on average, in spring, to 0.69 ± 0.21 (0.87) in autumn (Figure 2a). Contributions of net benthic metabolism to CO_2 outgassing varied among seasons, ranging from ~69% in summer, to ~22% in spring and autumn, to ~8% during the winter, but represented only about a third of the estimated mean annual CO_2 outgassing (Table 1). Assessments of net whole-stream metabolism (in mmol m^{-2} h^{-1}) using aquatic eddy covariance showed that half the reaches acted as CO_2 sinks (negative net whole-stream metabolism) in spring and summer. Overall, seasonal averages were negative and/or carbon neutral (-0.53 and -0.02; Figure 2a), being -20% and -30% of the CO_2 outgassing rates, respectively, on average. In contrast, in autumn and winter the net whole-stream metabolism was positive, but comprised only 25% (2.42 mmol m^{-2} h^{-1}) and 17% (1.81 mmol m^{-2} h^{-1}) of seasonal total outgassing of all streams, respectively. Outgassing of CO_2 was not correlated with the observed rates of net benthic or whole-stream metabolism, but was almost linearly proportional to stream discharge and baseflow (discharge normalized by the respective sub-catchment areas, power-law exponent 0.84 *versus* 1; Figure 2b, Table S1). Outgassing was maximal in autumn and winter under high discharge and lowest in summer. Porewater concentrations of CO_2 in the streambed and riparian soils of gaining reaches were comparable (Figure 2e). Overall, on the clay, the net benthic metabolism could account for 70% of the outgassed CO_2 in spring and all of CO_2 outgassing in summer (average of Priors and Sem sites in Table 1). In contrast, on the Chalk and Greensand, net benthic metabolism in spring and summer could only account on average for 8 to 10% of CO_2 outgassing at these sites, respectively (Table 1).

3.1.2 CH_4 fluxes, outgassing *versus* discharge and porewater concentrations

Outgassing of CH_4 (in mmol m^{-2} h^{-1}; mean ± se (median)) to the atmosphere ranged from 0.04 ± 0.02 (0.03) during summer, to 0.07 ± 0.03 (0.05) during autumn (Figure 2c). Chamber-based release of CH_4 from the sediments ranged from 0.37 ± 0.13 (0.23) in autumn, to 0.82 ± 0.24 (0.65) in winter (Figure 2c) and was up to 50 times higher than CH_4 outgassing (Figure 2c). The release of CH_4 from the streambed was also not correlated with CH_4 outgassing and revealed a non-linear relationship to normalized stream discharge (Figure 2d, Table S2). Porewater concentrations within the streambed and in bankside riparian soils in gaining reaches, were highly variable, but, overall, riparian CH_4 concentrations were four-fold lower (median to median) than in the streambed (Figure 2e). The release of CH_4 from the streambed (in μmol m^{-2} h^{-1}) showed large variation both across streams and seasons, but, overall, streambed sediments in the dark released significantly ($P < 0.001$, see Table S3) more CH_4 (median 23.8) than streambed sediments in the light (median 2.11, Figure 3). The only exception being the River Nadder on the Greensand, where the CH_4 release in the light was 7% higher than in the dark (Figure S3). Generally, mean sediment CH_4 release, quantified from on our data clustering approach, was highest on clay (up to 8.18, on average at night) and on sand streams (up to 18.5), with very little contribution from the Chalk gravels (up 0.04) (Figure 3). In contrast, vegetated patches of both Greensand and Chalk streambeds were found to be hotspots of CH_4 release (58.8).

3.2 High-resolution diel CO_2 and CH_4 outgassing in spring

We used high-resolution automated floating chambers to characterize diel dynamics of CO_2 and CH_4 outgassing. For CO_2, mean daytime outgassing (in mmol m^{-2} h^{-1}) ranged from 0.54 ± 0.02 (mean ± standard error) to 13.52 ± 0.35 across the six streams, while at night, outgassing was 30% higher, on average ($P = 0.036$, Figure 4a). Only 3.5% of the dataset (49 values) failed our quality check ($r^2<0.9$). Mean outgassing of CH_4 remained largely constant across the day, with no significant daytime to nighttime variability ($P = 0.455$; Figure 4b). Averaged daytime CH_4 outgassing (in μmol m^{-2} h^{-1}) ranged from 2.10 ± 0.05 to 56.82 ± 1,15. Increases in CO_2 outgassing at night tended to be greatest in streams on the Greensand and Chalk, where GPP tends to be the highest (e.g., average reach-scale estimates determined in 2013-14; Rovelli et al., 2017) despite its intrinsic temporal variability (see Hall, 2016; and references therein), and lowest on the more turbid clay streams, where

GPP also tends to be the lowest (Figure 4c). Discharge values (51 measurements, 3.5% of total) were mostly concomitant with those for CO_2.

Out of the total 1416 high-resolution chamber measurements, we only observed 21 ebullition events (i.e., 1.5%), and almost all exclusively at Priors (18 events, 86% of all events) on the clay. During these events, contributions from ebullition to total CH_4 outgassing (ebullition + diffusion), expressed as a percentage, was 13.5%, on average, ranging from no measured increase (33% of ebullition events) to 43% (1 event) and 73% (1 event) at River Ebble and West Avon, respectively. At River Nadder and Priors, the increase was found to be only 3% (1 event) and 9% (average of 18 events), respectively (Figure S9). Overall, ebullition had a very marginal effect on mean day and night CH_4 outgassing, with 0.7% at Priors, 0.5% at the Ebble, 0.3% at West Avon and a negligible 0.03% at the Nadder.

3.3 Methane oxidation potential and in-stream CH_4 turnover

Concentrations of suspended particulate matter ranged from 11 mg L^{-1} to 16 mg L^{-1} in Greensand streams in summer, up to 501 mg L^{-1} on the clay in autumn (Figure S5c). On average, suspended particulate matter was lowest on the Chalk (River Ebble; 88 ± 20 mg L^{-1}, mean ± standard error), intermediate on the Greensand (126 ± 58 and 129 ± 72 mg L^{-1} for River Nadder and West Avon, respectively) and highest on the clay (River Sem; 287 ± 91 mg L^{-1}). Laboratory-determined rates of potential methane oxidation ranged from 1.35 nmol L^{-1} h^{-1} for negligible (~0 mg L^{-1}) suspended particulate matter in the Greensand West Avon, to 32.22 nmol L^{-1} h^{-1} in the clay-based River Sem for 52 mg L^{-1} suspended particulate matter, with an overall robust correlation between methane oxidation and suspended particulate matter across all streams ($P < 0.001$, Figure S5). Rates of methane oxidation normalized to suspended particulate matter (in nmol mg^{-1} h^{-1}) were 0.98 ± 0.44, on average, and highest for Greensand streams (1.38 to 2.52) and lowest for the Chalk River Wylye (0.19). For the clay streams, methane oxidation activity was in between, although at the lower end (0.37 to 0.45). Concentrations of CH_4, normalized to suspended particulate matter, ranged from 3.82 to 53.64 nmol mg^{-1}, with no clear trend across geologies. Turnover of CH_4 in the water column via biological methane oxidation, quantified as R_{kCH4}, ranged from <0.01 to 0.22 h^{-1} and was 0.04 ± 0.01 (0.01) (mean ± standard error (median)), on average (Figure 4d). In contrast, turnover of CH_4 driven by gas transfer out of the streams (K_{CH4}) and flow driven dilution

(K_{flow}), were both substantially higher at 0.26 ± 0.02 (0.25) and 3.98 ± 0.57 (4.00) h^{-1}, respectively (Figure 4d).

3.4 Reach-scale mass balance modeling

3.4.1 Mean benthic CH_4 fluxes

The model was run with the mean benthic CH_4 fluxes from our logarithmic transformation and clustering approach. Mean estimates for average night and day fluxes (in µmol m^{-2} h^{-1}) were highest for the vegetated patches (night 58.78 and day 19.51) and lower, but still elevated, for the sandy patches (18.49 and 7.43) and for the clay streambed (8.18 and 4.32), respectively. For the gravel patch type, fluxes were strongly reduced at night (average 0.04) and turned negative, i.e. becoming sinks for CH_4 during the day (average -0.25).

3.4.2 Modelled reaches

Our model was applied to three of the reaches, representing the Chalk (River Wylye), Greensand (River Nadder) and clay (River Sem) during the summer. These sites were selected because they have been more extensively investigated with regards to O_2 fluxes (see Rovelli et al., 2017) which are used here to drive in-stream CO_2 dynamics. The model was run until day and night CO_2 and CH_4 concentrations reached steady-state and constant outgassing rates were achieved, which is illustrated in Figure 5b for the River Wylye. Overall, the model was able to reproduce the magnitude of observed CO_2 and CH_4 night outgassing rates at all three sites (Figure 5c). In terms of actual deviation from the observed day and night difference in outgassing, the model matched the dynamics in the Chalk and clay reaches (<3% deviation), but was found to underestimate diel outgassing in the Greensand reach by 20% (Figure 5d). In contrast, for CH_4, the Greensand model showed good agreement with the observations with only 4 % deviation. On the Chalk, the model could not initially reproduce the observed diel trends when contributions from the vegetated patches were scaled to their spatial coverage (51.5% of the reach), but was found to match the observations when a smaller fraction of this area (25%) was considered as a hotspot for CH_4 release. For the clay site, the model suggested a 4% difference between day and night outgassing of CH_4 which was at odds with the observed 21%. Due to the disproportionally

high standard error around the measured nighttime outgassing rate, this 21% difference was found to be not significant.

Modelling showed that, within the observed range of discharge, diel differences in CO_2 outgassing varied by up to 17% during the extremes of low flow and high flow (Table S4). Discharge, however, had a weaker effect (~6 % offset) on CH_4 than CO_2 at all sites. Temperature changes, exemplified by a 10% shift in mean temperature towards both lower nighttime and higher daytime averages, were found to change modelled outgassing for both gases by 6% to 9%. Changing the respiratory quotient from 0.8:1 to 1.2:1 (O_2:CO_2 equivalents), had only a minor effect (<7%). Small changes in suspended particulate matter (10% to 20%) also had very little effect (<1%) on modelled CH_4 outgassing, while peak (seasonal or annual) suspended particulate matter concentrations drove changes comparable in magnitude to those associated with changes in discharge. For the more turbid water of the clay and Greensand sites (River Sem and Nadder respectively) we also found that, under low flows, concentrations of suspended particulate matter ~240 mg L^{-1}, well below peak values, could potentially drive methane oxidation rates comparable in magnitude to the overall outgassing and effectively reducing daytime outgassing to 0 (Table S4). Values of *k* showed reduced variability across all three modeled reaches, increasing by about 50% between low discharge and high discharge conditions. When decoupled from discharge, such changes drove increases or decreases in outgassing that were on average 14% to 16%, for CH_4 and CO_2 across the sites. As the magnitude of both day and night outgassing are proportionally affected, the initial day-to-night ratio remained unchanged (Table S4).

4 Discussion

4.1 In-stream contributions to seasonal outgassing

The combined dataset from our array of flux measurement techniques revealed a marked difference in the magnitude of CO_2 and CH_4 outgassing compared to what could be accounted for by in-stream metabolism (Figure 2, Table 1). Given that our flux techniques integrate contrasting footprint areas, from patch-scale to km-long stream stretches, these results must be considered within a spatial context, in term of representativeness of in-stream dynamics. In Rovelli et al. (2018) we have shown for two of the investigated streams that benthic and whole-stream metabolism from based on aquatic eddy covariance were representative enough of in-stream dynamics to be combined with km-long assessments of O_2 water-air gas exchange (single station approach) to close the local O_2 budget regardless of

their spatial differences. As the same considerations for site selections was applied to each site, here and in Rovelli et al. (2017,2018), one could reasonably assume that in-stream dynamics were adequately represented within those measurements. Outgassing of CO_2 was strongly proportional to stream discharge (Figure 2b) indicating that catchment processes in the form of groundwater and soil water inputs are an important overall controlling factor (Butman & Raymond, 2011; Marx et al., 2017). The relative contributions of each input have not been quantified in this study but soil-derived CO_2 inputs from shallow lateral subsurface flows are likely to be relatively more important at the clay sites compared to the groundwater-fed streams on the Chalk and Greensand. Given the high proportion of groundwater-derived baseflow throughout the year in the Chalk sites (90%, exemplified in Figure S1c) it seems likely that, for these streams, CO_2 derived from deeper groundwater sources dominate inputs. The lack of a similar relationship for CH_4 outgassing suggests other factors contribute, including local streambed sources of CH_4 , that we know have a high potential to produce CH_4 (Bodmer et al., 2020; Crawford & Stanley, 2016; Romeijn et al., 2019; Sanders et al., 2007; Schindler & Krabbenhoft, 1998; Shelley et al., 2015). Further inputs might arise also from proportional changes in the upstream contributions of CH_4 in different flow pathways (e.g., under baseflow and quickflow). Although CO_2 outgassing could be predicted much better by discharge than by net benthic metabolism, all the streambeds were typically net heterotrophic (with the exception, in spring, of the Ebble on the Chalk and the Nadder on the Greensand), acting as sources of both CO_2 and CH_4 to the streams (Figure 2). In spring and summer, half the reaches acted as CO_2 sinks (negative net whole-stream metabolism, illustrating the important control that photosynthetic activity exerts on carbon dynamics in these lowland, headwater streams (Figure 2, Table 1). During autumn and winter, net whole-stream metabolism was positive, but still more than 80% of the CO_2 outgassing was attributable to transport in from the catchment. Thus, even though overall the streambeds act as CO_2 sources (yearly median 0.57 mmol m^{-2} d^{-1}), the majority of CO_2 appears catchment-derived (see Hotchkiss et al., 2015), but seasonal dynamics in CO_2 outgassing are modulated by in-stream metabolism.

4.2 Modulation of outgassing from catchment geology

In addition to the broad, overall patterns in CO_2 outgassing and discharge, i.e., averages across all six streams in Figure 2, there was also variation in sources and sinks in relation to underlying catchment geology. Elsewhere, we have shown that dynamics in net

whole-stream metabolism were distinctive across these geologies, with clay reaches largely representing biological sources of CO_2, Chalk reaches typically representing CO_2 sinks, and the Greensand shifting from sinks for CO_2 in spring, to sources throughout the rest of the year (Rovelli et al., 2017). On the clay, we found that a large portion of CO_2 outgassing in spring could be accounted by the net benthic metabolism, while in summer, the totality of outgassed CO_2 could be attributed to streambed metabolism. In contrast, streambed metabolism on the Chalk and Greensand could only account for up to 13% of the total outgassing (Table 1), indicating that while carbonate-rich groundwater inputs are significant sources of CO_2 to groundwater-fed streams on Chalk and Greensand (Gallois & Owen, 2018), such contribution is minimal in impermeable clay streams.

4.3 Diel dynamics

Our high-temporal-resolution measurements (spring 2015) showed a clear decrease in CO_2 outgassing during the day across all streams. Such a diel pattern is consistent with the modulation of CO_2 concentration from in-stream metabolism (i.e., streambed, water column and riparian zone) which offsets CO_2 concentrations towards higher values *via* respiration at night and towards lower values *via* net primary production during the day (Herreid et al., 2020; Hotchkiss et al., 2015; Lynch et al., 2010; Rocher-Ros et al., 2020). Our mean CO_2 outgassing rates were consistent with those reported by Attermeyer et al. (2021) for a collection of 34 European rivers (median up to 25.6 mmol m^{-2} h^{-1}) including 13 headwaters (stream order 1-3; median up to 20.5 mmol m^{-2} h^{-1}), where drifting flux chambers were used on a seasonal basis. Our results are also in line with their overall reported increase of 39% and 24% between midday and nighttime CO_2 outgassing (all seasons combined and summertime only respectively). Comparable findings were also reported from empirical models (e.g., Gómez-Gener et al., (2021)), where the authors reported an overall 27% diel difference in outgassing based on long-term monitoring of over 66 streams worldwide.

For CH_4, the magnitude of our chamber-based estimates of outgassing are representative of the global averages for headwaters presented by Stanley et al. (2016) based on a large (n=205) database of headwater streams, which includes estimates for other lowland headwaters in temperate climates (e.g., Hlaváčová et al., 2006). In contrast to our observations for CO_2, diel CH_4 outgassing remained constant (Figure 4) and was thus at odds with the approximate doubling of CH_4 released from the sediments between dark and light chambers (Figure 3). This suggests that before being outgassed through re-aeration, CH_4

released from strong sources such as vegetated sediments could: (i) be diluted within the water column by water with a lower concentration of CH_4 (immediate surroundings and upstream); and/or (ii) be oxidized in the water column, especially in the more turbid streams on the clay and Greensand (Rovelli et al., 2017; Sawakuchi et al., 2016). We tested these hypotheses by comparing the turnover time for CH_4 in the stream associated with outgassing (K_{CH4}), with turnover due to methane oxidation in the water column (Rk_{CH4}) and flow-driven dilution (K_{flow}). A ratio of Rk_{CH4} to K_{CH4} higher than 1, for example, would indicate that methane oxidation plays a major role modulating CH_4 concentration changes in the water column. As shown in Figure 5, however, the potential for CH_4 to be removed by methane oxidation in the water column is trivial compared to outgassing through re-aeration. Here the ratio was consistently < 0.2 (median) and would only approach 1 when suspended particulate matter concentrations exceed 300 to 400 mg L^{-1}, which only occurred during brief periods of intense rainfall during our study (see Figures S1 and S5). The influence of methane oxidation in the water column would be even lower for CH_4 transported rapidly through the water column by ebullition (McGinnis et al., 2016). In this study, our analysis of the high-resolution outgassing dataset showed very little evidence of ebullition events, and their effect on the overall outgassing rates was found to be minimal (Figure S9). The likely reason for this is that porewater CH_4 concentrations in our streambed sediments were just too low for widespread development of CH_4 bubbles in the sediment (median CH_4 concentrations = 0.718 µmol L^{-1}, Figure 1e, in our streambeds c.f. 1000s µmol L^{-1} CH_4 reported by McGinnis et al. (2016) for a stream where ebullition was identified as the main driver of CH_4 outgassing). In the absence of strong ebullition, the turnover of CH_4 in the water column will likely be determined by the interplay of K_{CH4} and K_{flow}. Across sites, the ratio of K_{flow} to K_{CH4} was, on average, 15 to 1, indicating that dilution by stream flow likely impresses the dominant control on in-stream CH_4 concentrations and their temporal variability.

To further rationalize the differences that we observed between the day and night outgassing rates for CH_4 and CO_2, we applied our mass-balance model to three reaches, ranging from a fast-flowing highly-productive clear-water stream on the Chalk (River Wylye) to a slow-flowing turbid stream on the clay (River Sem), with the River Nadder on the Greensand representing an intermediate system. On the Chalk, despite large CO_2 import from the groundwater-fed catchment and enhanced dilution from high flow, we expected in-stream metabolism (i.e., net benthic and whole-stream metabolism) to exert a clear modulation on diel variability in CO_2 outgassing. On the Clay, conversely, we expected to have the best

chance of detecting diel changes in CH_4 outgassing, as here we observed strong streambed CH_4 release in combination with the highest ratio of Rk_{CH4} to K_{flow} of all sites.

Despite the recognized simplicity of our model (see Methods), we were mostly able to reproduce the contrasting diel patterns that we observed for CO_2 and CH_4 in the field (Figure 5c,d), thus further validating the representativeness of our assessment of in-stream metabolism. For CO_2, the largest deviation from the observed outgassing rates was found on the Greensand; likely a result of under-representation of the heterogeneity of the sand patch type. Whilst the majority of CO_2 in the stream water is transported in from the catchment (Butman & Raymond, 2011; Hotchkiss et al., 2015), primary production, and respiration at the reach scale during the summer months, significantly split the resulting CO_2 outgassing between night and day (Figure 4, Figure 5). Later in the year, in autumn and/or winter, these streams turn into biological sources of CO_2, i.e., positive net whole-stream metabolism (see Rovelli et al., 2017) likely making decreases in daytime CO_2 concentration from gross primary production less pronounced, thus dampening the overall diel CO_2 dynamics.

In contrast, CH_4 present in the stream water is predominantly produced in the streambed, with the magnitude of production depending on sediment type (Jones & Mulholland, 1998a; Shelley et al., 2015) (Figure 3a). Release of CH_4 from a streambed can be less during the day, most likely due to diel changes in microphytobenthic O_2 production on the immediate streambed (Fenchel & Glud, 2000) and deeper hyporheic, temperature-modulated microbial metabolism (e.g., Mächler et al., 2013). The main challenge when quantifying CH_4 benthic release at the reach scale remains the integration of the contributions from hotspots, e.g. fine sediment accumulated under vegetation (see Sanders et al., 2007). Such hotspots (such as *Ranunculus* patches in chalk rivers) are heterogeneous in terms of both sediment depth and areal extent, and change in shape and volume with the seasonal growth and die-back of vegetation (Cotton et al., 2006; Sanders et al., 2007). On the Chalk River Wylye, we found that only 25% of the contributions from the observed vegetated patch area were needed to provide a good model fit to our observational data, with higher percentage contributions resulting in an over-estimate of reach-scale benthic CH_4 release. This suggests that these fine-sediment patches might be more heterogeneous in terms of CH_4 release than we were able to resolve with our patch-scale measurements.

In general, we found that once released into the water column, the overall sediment CH_4 signal is diluted and dissipated by stream flow, rather than by biologically mediated

methane oxidation in the water column; and the resulting space and time integrated CH_4 outgassing rates to the atmosphere remain comparatively constant between day and night (Figure 4, Figure 5). It should also be noted that the highest R_{KCH4} values, driven by the highest methane oxidation activity, occurred during periods of intense rainfall, when suspended particulate matter concentrations were high and discharge elevated above baseflow. As a result, K_{flow} and likely K_{CH4} would both be enhanced, with the overall effect of methane oxidation on CH_4 dynamics being even further dampened, as shown by our model (see Table S4). In contrast, regions of reduced flows within a stream (e.g., pools and marginal regions) or periods of strongly reduced flow (e.g., during summertime droughts) would enhance R_{KCH4} locally and thus increase the importance of methane oxidation to water column CH_4 dynamics. In terms of emissions, however, such conditions would also reduce re-aeration (K_{CH4}), and the concentration of CH_4 in the water column, thus strongly limiting the overall outgassing of CH_4 from the reach, as illustrated in our model for the more turbid streams (clay and Greensand, Table S4).

5 Conclusions

Here we have characterized distinct biophysical controls on the final outgassing of CO_2 and CH_4 from headwater streams in lowland catchments. Outgassed CO_2 is principally controlled by hydrology – tempered by season and whole stream metabolism – stressing the importance of the connection between terrestrial and freshwater ecosystems with regard to carbon cycling. In contrast, outgassed CH_4 is principally stream borne and, once released from sediment, that CH_4 passes relatively unimpeded by biology in the water column, with dilution largely governing the final integrated magnitude of CH_4 outgassing. Our observations have characterized distinct biophysical controls on the two carbon gases and incorporating the intense carbon cycling of headwater streams into the global carbon cycle will require distinct parameterizations for each carbon gas in Earth system models.

Acknowledgments

This study was financially supported through the Natural Environment Research Council (NERC) Macronutrient Cycles Programme (grant numbers NE/J012106/1, MT, and

NE/J011738/1, AB), the German Science Foundation (grant RO 5921/1-1, LR). This work was funded by HADES-ERC Advanced Grant (No. 669947), the FNU-7014-00078 grant and the Danish National Research Foundation through the Danish Center for Hadal Research, HADAL (No. DNRF145) awarded to R.N. Glud. We acknowledge the land owners for allowing us access to the streams and thanks E. Malone, A. Jones, S. Warren, I. Sanders, F. Shelley and V. Warren for help with sample collection and preparation. Data presented in this work are available from NERC Environmental Information Data Centre.

Additional information

Supplementary information is available in the online version of the paper.

References

Allen, D. J., Darling, W. G., Davies, J., Newell, A. J., Gooddy, D. C., & Collins, A. L. (2014). Groundwater conceptual models: implications for evaluating diffuse pollution mitigation measures. *Quarterly Journal of Engineering Geology and Hydrogeology*, *47*(1), 65–80. https://doi.org/10.1144/qjegh2013-043

Attard, K. M., Stahl, H., Kamenos, N. A., Turner, G., Burdett, H. L., & Glud, R. N. (2015). Benthic oxygen exchange in a live coralline algal bed and an adjacent sandy habitat: an eddy covariance study. *Marine Ecology Progress Series*, *535*, 99–115. https://doi.org/10.3354/meps11413

Attermeyer, K., Casas-Ruiz, J. P., Fuss, T., Pastor, A., Cauvy-Fraunié, S., Sheath, D., et al. (2021). Carbon dioxide fluxes increase from day to night across European streams. *Communications Earth & Environment*, *2*(1), 118. https://doi.org/10.1038/s43247-021-00192-w

Barton, K. (2009). Multi-model inference. R Package Version 1.43.15. Retrieved from http://r-forge.r-project.org/projects/mumin/

Bastviken, D., Tranvik, L. J., Downing, J. A., Crill, P. M., & Enrich-Prast, A. (2011). Freshwater Methane Emissions Offset the Continental Carbon Sink. *Science*, *331*(6013), 50–50. https://doi.org/10.1126/science.1196808

Bastviken, D., Sundgren, I., Natchimuthu, S., Reyier, H., & Gålfalk, M. (2015). Technical Note: Cost-efficient approaches to measure carbon dioxide (CO_2) fluxes and concentrations in terrestrial and aquatic environments using mini loggers. *Biogeosciences*, *12*(12), 3849–3859. https://doi.org/10.5194/bg-12-3849-2015

Bates, D., Mächler, M., Bolker, B. M., & Walker, S. C. (2015). Fitting linear mixed-effects models using lme4. *Journal of Statistical Software*. https://doi.org/10.18637/jss.v067.i01

Battin, T. J., Luyssaert, S., Kaplan, L. A., Aufdenkampe, A. K., Richter, A., & Tranvik, L. J. (2009). The boundless carbon cycle. *Nature Geoscience*, *2*(9), 598–600. https://doi.org/10.1038/ngeo618

Berg, P., & Pace, M. L. (2017). Continuous measurement of air–water gas exchange by underwater eddy covariance. *Biogeosciences*, *14*(23), 5595–5606. https://doi.org/10.5194/bg-14-5595-2017

Berg, P., Roy, H., Janssen, F., Meyer, V., Jorgensen, B. B., Huettel, M., & de Beer, D. (2003). Oxygen uptake by aquatic sediments measured with a novel non-invasive eddy-correlation technique. *Marine Ecology Progress Series*, *261*, 75–83. https://doi.org/10.3354/meps261075

Berg, P., Roy, H., & Wiberg, P. L. (2007). Eddy correlation flux measurements: The sediment surface area that contributes to the flux. *Limnology and Oceanography*, *52*(4), 1672–1684. https://doi.org/10.4319/lo.2007.52.4.1672

Bodmer, P., Wilkinson, J., & Lorke, A. (2020). Sediment Properties Drive Spatial Variability of Potential Methane Production and Oxidation in Small Streams. *Journal of Geophysical Research: Biogeosciences*, *125*(1). https://doi.org/10.1029/2019JG005213

Bristow, C. R., Barton, C. M., Westhead, R. K., Freshney, E. C., Cox, B. M., & Woods, M. A. (1999). *The Wincanton district - a concise account of the geology*. *The Wincanton district - a concise account of the geology. Memoir for 1:50 000 Geological Sheet 297 (England and Wales)*.

Butman, D., & Raymond, P. A. (2011). Significant efflux of carbon dioxide from streams and rivers in the United States. *Nature Geoscience*, *4*(12), 839–842. https://doi.org/10.1038/ngeo1294

Ciais, P., Sabine, C., Bala, G., Bopp, L., Brovkin, V., Canadell, J., et al. (2013). Carbon and Other Biogeochemical Cycles. In Intergovernmental Panel on Climate Change (Ed.), *Climate Change 2013 - The Physical Science Basis* (pp. 465–570). Cambridge: Cambridge University Press. https://doi.org/10.1017/CBO9781107415324.015

Cole, J. J., Prairie, Y. T., Caraco, N. F., McDowell, W. H., Tranvik, L. J., Striegl, R. G., et al. (2007). Plumbing the global carbon cycle: Integrating inland waters into the terrestrial carbon budget. *Ecosystems*, *10*(1), 171–184. https://doi.org/10.1007/s10021-006-9013-8

Cotton, J. A., Wharton, G., Bass, J. A. B., Heppell, C. M., & Wotton, R. S. (2006). The effects of seasonal changes to in-stream vegetation cover on patterns of flow and accumulation of sediment. *Geomorphology*, *77*(3–4), 320–334. https://doi.org/10.1016/j.geomorph.2006.01.010

Crawford, J. T., & Stanley, E. H. (2016). Controls on methane concentrations and fluxes in streams draining human-dominated landscapes. *Ecological Applications*, *26*(5), 1581–1591. https://doi.org/10.1890/15-1330

Dalsgaard, T. (ed), Nielsen, L. P., Brotos, V., Viaroli, P., Underwood, G., Nedwell, D. B., et al. (2000). *Protocol handbook for NICE-Nitrogen Cycling in Estuaries: a project under the EU research programme: Marine Science and Technology (Mast III)*. *National Environmental Research Institute*.

Fenchel, T., & Glud, R. N. (2000). Benthic primary production and O 2 -CO 2 dynamics in a shallow-water sediment: Spatial and temporal heterogeneity. *Ophelia*, *53*(2), 159–171. https://doi.org/10.1080/00785236.2000.10409446

Gallois, R., & Owen, H. (2018). The stratigraphy of the mid Cretaceous (Albian) Upper Greensand Formation

of the Wessex Basin and South West England, UK. *Acta Geologica Polonica*, *68*(2), 161–180. https://doi.org/10.1515/agp-2018-0003

Glud, R. N. (2008). Oxygen dynamics of marine sediments. *Marine Biology Research*, *4*(4), 243–289. https://doi.org/10.1080/17451000801888726

Gómez-Gener, L., Rocher-Ros, G., Battin, T., Cohen, M. J., Dalmagro, H. J., Dinsmore, K. J., et al. (2021). Global carbon dioxide efflux from rivers enhanced by high nocturnal emissions. *Nature Geoscience*, *14*(5), 289–294. https://doi.org/10.1038/s41561-021-00722-3

Gurnell, A., Angold, P., & Edwards, P. (1996). Extracting information from river corridor surveys. *Applied Geography*, *16*(1), 1–19. https://doi.org/10.1016/0143-6228(95)00022-4

Hall, R. O. (2016). Metabolism of Streams and Rivers. In *Stream Ecosystems in a Changing Environment* (pp. 151–180). Elsevier. https://doi.org/10.1016/B978-0-12-405890-3.00004-X

Heppell, C. M., & Binley, A. (2016a). Hampshire Avon: Vertical head gradient, saturated hydraulic conductivity and pore water chemistry data from six river reaches. *NERC Environmental Information Data Centre*. https://doi.org/10.5285/d82a04ce-f04d-40b4-9750-1a2bf7dc29a3

Heppell, C. M., & Binley, A. J. (2016b). Hampshire Avon: Daily discharge, stage and water chemistry data from four tributaries (Sem, Nadder, West Avon, Ebble). *NERC Environmental Information Data Centre*. https://doi.org/10.5285/0dd10858-7b96- 41f1-8db5-e7b4c4168af5

Heppell, C. M. ., & Parker, S. J. (2018). Hampshire Avon: Dissolved oxygen data collected at one minute intervals from five river reaches. *NERC Environmental Information Data Centre*. https://doi.org/10.5285/840228a7-40a1-4db4-aef0-a9fea2079987

Heppell, Catherine M., Binley, A., Trimmer, M., Darch, T., Jones, A., Malone, E., et al. (2017). Hydrological controls on DOC : nitrate resource stoichiometry in a lowland, agricultural catchment, southern UK. *Hydrology and Earth System Sciences*, *21*(9), 4785–4802. https://doi.org/10.5194/hess-21-4785-2017

Herreid, A. M., Wymore, A. S., Varner, R. K., Potter, J. D., & McDowell, W. H. (2020). Divergent Controls on Stream Greenhouse Gas Concentrations Across a Land-Use Gradient. *Ecosystems*. https://doi.org/10.1007/s10021-020-00584-7

Hlaváčová, E., Rulík, M., Čáp, L., & Mach, V. (2006). Greenhouse gas (CO_2, CH_4, N_2O) emissions to the atmosphere from a small lowland stream in Czech Republic. *Archiv Für Hydrobiologie*, *165*(3), 339–353. https://doi.org/10.1127/0003-9136/2006/0165-0339

Hotchkiss, E. R., Hall Jr, R. O., Sponseller, R. A., Butman, D., Klaminder, J., Laudon, H., et al. (2015). Sources of and processes controlling CO_2 emissions change with the size of streams and rivers. *Nature Geoscience*, *8*(9), 696–699. https://doi.org/10.1038/ngeo2507

Jarvie, H. P., Jürgens, M. D., Williams, R. J., Neal, C., Davies, J. J. L., Barrett, C., & White, J. (2005). Role of river bed sediments as sources and sinks of phosphorus across two major eutrophic UK river basins: the Hampshire Avon and Herefordshire Wye. *Journal of Hydrology*, *304*(1–4), 51–74. https://doi.org/10.1016/j.jhydrol.2004.10.002

Jones, J. B., & Mulholland, P. J. (1998a). Influence of drainage basin topography and elevation on carbon dioxide and methane supersaturation of stream water. *Biogeochemistry*, *40*, 57–72. https://doi.org/10.1023/A:1005914121280

Jones, J. B., & Mulholland, P. J. (1998b). Methane input and evasion in a hardwood forest stream: Effects of subsurface flow from shallow and deep pathways. *Limnology and Oceanography*. https://doi.org/10.4319/lo.1998.43.6.1243

Koopmans, D. J., & Berg, P. (2015). Stream oxygen flux and metabolism determined with the open water and aquatic eddy covariance techniques. *Limnology and Oceanography*, *60*(4), 1344–1355. https://doi.org/10.1002/lno.10103

Lansdown, K., McKew, B. A., Whitby, C., Heppell, C. M., Dumbrell, A. J., Binley, A., et al. (2016). Importance and controls of anaerobic ammonium oxidation influenced by riverbed geology. *Nature Geosci*, *9*(5), 357–360. https://doi.org/10.1038/ngeo2684

Lenth, R. V. (2019). Emmeans: Estimated Marginal Means, aka Least-Squares Means. R package version 1.4.5. Retrieved from https://cran.r-project.org/web/packages/emmeans/

Li, M., Peng, C., Zhang, K., Xu, L., Wang, J., Yang, Y., et al. (2021). Headwater stream ecosystem: an important source of greenhouse gases to the atmosphere. *Water Research*, *190*, 116738. https://doi.org/10.1016/j.watres.2020.116738

Lorke, A., Bodmer, P., Noss, C., Alshboul, Z., Koschorreck, M., Somlai-Haase, C., et al. (2015). Technical note: drifting versus anchored flux chambers for measuring greenhouse gas emissions from running waters. *Biogeosciences*, *12*(23), 7013–7024. https://doi.org/10.5194/bg-12-7013-2015

Lorrai, C., McGinnis, D. F., Berg, P., Brand, A., & Wuest, A. (2010). Application of Oxygen Eddy Correlation in Aquatic Systems. *Journal of Atmospheric and Oceanic Technology*, *27*(9), 1533–1546. https://doi.org/10.1175/2010JTECHO723.1

Lynch, J. K., Beatty, C. M., Seidel, M. P., Jungst, L. J., & DeGrandpre, M. D. (2010). Controls of riverine CO 2

over an annual cycle determined using direct, high temporal resolution p CO 2 measurements. *Journal of Geophysical Research*, *115*(G3), G03016. https://doi.org/10.1029/2009JG001132

Mächler, L., Brennwald, M. S., & Kipfer, R. (2013). Argon Concentration Time-Series As a Tool to Study Gas Dynamics in the Hyporheic Zone. *Environmental Science & Technology*, *47*(13), 7060–7066. https://doi.org/10.1021/es305309b

Marx, A., Dusek, J., Jankovec, J., Sanda, M., Vogel, T., van Geldern, R., et al. (2017). A review of CO 2 and associated carbon dynamics in headwater streams: A global perspective. *Reviews of Geophysics*, *55*(2), 560–585. https://doi.org/10.1002/2016RG000547

McGinnis, D. F., Cherednichenko, S., Sommer, S., Berg, P., Rovelli, L., Schwarz, R., et al. (2011). Simple, robust eddy correlation amplifier for aquatic dissolved oxygen and hydrogen sulfide flux measurements. *Limnology and Oceanography-Methods*, *9*, 340–347. https://doi.org/10.4319/lom.2011.9.340

McGinnis, D. F., Bilsley, N., Schmidt, M., Fietzek, P., Bodmer, P., Premke, K., et al. (2016). Deconstructing Methane Emissions from a Small Northern European River: Hydrodynamics and Temperature as Key Drivers. *Environmental Science & Technology*, *50*(21), 11680–11687. https://doi.org/10.1021/acs.est.6b03268

Miles, B. W. J., Stokes, C. R., Vieli, A., & Cox, N. J. (2013). Rapid, climate-driven changes in outlet glaciers on the Pacific coast of East Antarctica. *Nature*. https://doi.org/10.1038/nature12382

Millero, F. J. (1979). The thermodynamics of the carbonate system in seawater. *Geochimica et Cosmochimica Acta*, *43*(10), 1651–1661. https://doi.org/10.1016/0016-7037(79)90184-4

Murniati, E., Geissler, S., & Lorke, A. (2015). Short-term and seasonal variability of oxygen fluxes at the sediment–water interface in a riverine lake. *Aquatic Sciences*, *77*(2), 183–196. https://doi.org/10.1007/s00027-014-0362-7

Myhre, G., Shindell, D., Bréon, F., Collins, W., Fuglestvedt, J., Huang, J., et al. (2013). *Anthropogenic and natural radiative forcing. In: Climate change 2013: the physical science basis. Contribution of working group I. Climate Change 2013 - The Physical Science Basis*.

Peter, H., Singer, G. A., Preiler, C., Chifflard, P., Steniczka, G., & Battin, T. J. (2014). Scales and drivers of temporal p CO 2 dynamics in an Alpine stream. *Journal of Geophysical Research: Biogeosciences*, *119*(6), 1078–1091. https://doi.org/10.1002/2013JG002552

Pinheiro, J. C., & Bates, D. M. (2000). *Mixed-Effects Models in S and S-PLUS*. *Mixed-Effects Models in S and S-PLUS*. New York: Springer-Verlag. https://doi.org/10.1007/b98882

Podgrajsek, E., Sahlee, E., Bastviken, D., Holst, J., Lindroth, A., Tranvik, L., & Rutgersson, A. (2014). Comparison of floating chamber and eddy covariance measurements of lake greenhouse gas fluxes. *Biogeosciences*, *11*(15), 4225–4233. https://doi.org/10.5194/Bg-11-4225-2014

R Core Team. (2014). R Core Team (2014). R: A language and environment for statistical computing. *R Foundation for Statistical Computing, Vienna, Austria. URL Http://Www.R-Project.Org/*.

Raymond, P. A., Zappa, C. J., Butman, D., Bott, T. L., Potter, J., Mulholland, P., et al. (2012). Scaling the gas transfer velocity and hydraulic geometry in streams and small rivers. *Limnology and Oceanography: Fluids and Environments*, *2*(1), 41–53. https://doi.org/10.1215/21573689-1597669

Raymond, P. A., Hartmann, J., Lauerwald, R., Sobek, S., McDonald, C., Hoover, M., et al. (2013). Global carbon dioxide emissions from inland waters. *Nature*, *503*(7476), 355–359. https://doi.org/10.1038/nature12760

Reiman, J., & Xu, Y. (2018). Diel Variability of pCO_2 and CO_2 Outgassing from the Lower Mississippi River: Implications for Riverine CO_2 Outgassing Estimation. *Water*, *11*(1), 43. https://doi.org/10.3390/w11010043

Revsbech, N. P. (1989). An oxygen microelectrode with a guard cathode. *Limnology and Oceanography*, *34*(2), 474–478. https://doi.org/10.4319/lo.1989.34.2.0474

Rocher-Ros, G., Sponseller, R. A., Bergström, A., Myrstener, M., & Giesler, R. (2020). Stream metabolism controls diel patterns and evasion of CO 2 in Arctic streams. *Global Change Biology*, *26*(3), 1400–1413. https://doi.org/10.1111/gcb.14895

Romeijn, P., Comer-Warner, S. A., Ullah, S., Hannah, D. M., & Krause, S. (2019). Streambed Organic Matter Controls on Carbon Dioxide and Methane Emissions from Streams. *Environmental Science & Technology*, *53*(5), 2364–2374. https://doi.org/10.1021/acs.est.8b04243

Rovelli, L., Attard, K. M., Binley, A., Heppell, C. M., Stahl, H., Trimmer, M., & Glud, R. N. (2017). Reach-scale river metabolism across contrasting sub-catchment geologies: Effect of light and hydrology. *Limnology and Oceanography*, *62*(S1), S381–S399. https://doi.org/10.1002/lno.10619

Rovelli, L., Attard, K. M., Heppell, C. M., Binley, A., Trimmer, M., & Glud, R. N. (2018). Headwater gas exchange quantified from O 2 mass balances at the reach scale. *Limnology and Oceanography: Methods*, *16*(10), 696–709. https://doi.org/10.1002/lom3.10281

Rovelli, L., Olde, L. A., Heppell, C. M., Binley, A., Yvon Durocher, G., Glud, R. N., & Trimmer, M. . et al. (2021a). High-resolution time series of day and night outgassing rates of carbon dioxide and methane for

six tributaries of Hampshire River Avon (UK) collected with an automated floating chamber in late spring 2015. *Figshare. Dataset*. https://doi.org/10.6084/m9.figshare.16545954.v1

Rovelli, L., Olde, L. A., Heppell, C. M., Binley, A., Yvon Durocher, G., Glud, R. N., & Trimmer, M. (2021b). Summary data of chamber-based oxygen and methane consumption and production in the streambed and outgassing of carbon dioxide and methane to the atmosphere collected seasonally for six tributaries of Hampshire River Avon (UK) during 2013-2014. *Figshare. Dataset*. https://doi.org/10.6084/m9.figshare.16545846.v1

Rovelli, L. ., Attard, K. M. ., Stahl, H. ., & Glud, R. N. . (2016). Summary data of reach scale oxygen consumption and production in the streambed and in the water column at six tributaries of Hampshire River Avon collected seasonally in 2013 to 2014. *NERC Environmental Information Data Centre*.

Sanders, I. A., Heppell, C. M., Cotton, J. A., Wharton, G., Hildrew, A. G., Flowers, E. J., & Trimmer, M. (2007). Emission of methane from chalk streams has potential implications for agricultural practices. *Freshwater Biology*, *52*(6), 1176–1186. https://doi.org/10.1111/j.1365-2427.2007.01745.x

Sawakuchi, H. O., Bastviken, D., Sawakuchi, A. O., Ward, N. D., Borges, C. D., Tsai, S. M., et al. (2016). Oxidative mitigation of aquatic methane emissions in large Amazonian rivers. *Global Change Biology*, *22*(3), 1075–1085. https://doi.org/10.1111/gcb.13169

Schindler, J. E., & Krabbenhoft, D. P. (1998). The hyporheic zone as a source of dissolved organic carbon and carbon gases to a temperate forested stream. *Biogeochemistry*, *43*(2), 157–174. https://doi.org/10.1023/A:1006005311257

Shelley, F., Grey, J., & Trimmer, M. (2014). Widespread methanotrophic primary production in lowland chalk rivers. *Proceedings of the Royal Society B: Biological Sciences*, *281*(1783), 20132854–20132854. https://doi.org/10.1098/rspb.2013.2854

Shelley, F., Abdullahi, F., Grey, J., & Trimmer, M. (2015). Microbial methane cycling in the bed of a chalk river: oxidation has the potential to match methanogenesis enhanced by warming. *Freshwater Biology*, *60*(1), 150–160. https://doi.org/10.1111/fwb.12480

Stanley, E. H., Casson, N. J., Christel, S. T., Crawford, J. T., Loken, L. C., & Oliver, S. K. (2016). The ecology of methane in streams and rivers: patterns, controls, and global significance. *Ecological Monographs*, *86*(2), 146–171. https://doi.org/10.1890/15-1027

Stets, E. G., Butman, D., McDonald, C. P., Stackpoole, S. M., DeGrandpre, M. D., & Striegl, R. G. (2017). Carbonate buffering and metabolic controls on carbon dioxide in rivers. *Global Biogeochemical Cycles*, *31*(4), 663–677. https://doi.org/10.1002/2016GB005578

Striegl, R. G., Dornblaser, M. M., McDonald, C. P., Rover, J. R., & Stets, E. G. (2012). Carbon dioxide and methane emissions from the Yukon River system. *Global Biogeochemical Cycles*, *26*(4). https://doi.org/10.1029/2012GB004306

Therkildsen, M. S., & Lomstein, B. A. (1993). Seasonal variation in net benthic C-mineralization in a shallow estuary. *FEMS Microbiology Ecology*, *12*(2), 131–142. https://doi.org/10.1111/j.1574-6941.1993.tb00025.x

Trimmer, M., Sanders, I. . A., & Heppell, C. . M. (2009). Carbon and nitrogen cycling in a vegetated lowland chalk river impacted by sediment. *Hydrological Processes*, *23*(15), 2225–2238. https://doi.org/10.1002/Hyp.7276

Trimmer, M., Maanoja, S., Hildrew, A. G., Pretty, J. L., & Grey, J. (2010). Potential carbon fixation via methane oxidation in well-oxygenated river bed gravels. *Limnology and Oceanography*, *55*(2), 560–568. https://doi.org/10.4319/lo.2010.55.2.0560

Weiss, R. F. (1974). Carbon dioxide in water and seawater: the solubility of a non-ideal gas. *Marine Chemistry*, *2*(3), 203–215. https://doi.org/10.1016/0304-4203(74)90015-2

Wiesenburg, D. A., & Guinasso, N. L. (1979). Equilibrium solubilities of methane, carbon monoxide, and hydrogen in water and sea water. *Journal of Chemical & Engineering Data*, *24*(4), 356–360. https://doi.org/10.1021/je60083a006

Yamamoto, S., Alcauskas, J. B., & Crozier, T. E. (1976). Solubility of methane in distilled water and seawater. *Journal of Chemical & Engineering Data*, *21*(1), 78–80. https://doi.org/10.1021/je60068a029

Yu, Z., Wang, D., Li, Y., Deng, H., Hu, B., Ye, M., et al. (2017). Carbon dioxide and methane dynamics in a human-dominated lowland coastal river network (Shanghai, China). *Journal of Geophysical Research: Biogeosciences*, *122*(7), 1738–1758. https://doi.org/10.1002/2017JG003798

Zuur, A. F., Ieno, E. N., Walker, N., Saveliev, A. A., & Smith, G. M. (2009). *Mixed effects models and extensions in ecology with R*. New York, NY: Springer New York. https://doi.org/10.1007/978-0-387-87458-6

Tables

Table 1. Percentage of CO_2 outgassing rate (CO_2out) that could potentially be accounted for by either net benthic metabolism (NBM) or whole-stream ecosystem metabolism (NWM). The percentages are based on flux comparisons by season and stream, and would only equal 100% if the amount of CO_2 outgassing is matched by that of local metabolism, i.e., NBM or NWM. Note that negative values indicate net sinks for CO_2, e.g., in the Nadder in spring, net benthic metabolism represents the potential to reduce CO_2 outgassing by 17%.

Contributions	Season	Priors (Clay)	Sem (Clay)	Ebble (Chalk)	Wylye (Chalk)	West Avon (Greensand)	Nadder (Greensand)	Seasonal average (%)
NBM / CO_2out	Spring	91	46	-3	9	4	-17	22
	Summer	103	234	10	17	15	39	70
	Autumn	20	20	6	82	0	9	23
	Winter	6	19	-[a]	1	-[a]	7	8
NWM / CO_2out	Spring	23	6	-52	-8	22	-113	-20
	Summer	-18	115	54	390	0	26	-36
	Autumn	1	107	36	-56	-[a]	38	25
	Winter	9	29	-[a]	3	-[a]	28	17

[a]: site not accessible due to flooding.

Figures caption

Figure 1. Study sites and experimental setup. (a) Map of the Hampshire River Avon showing geology and our six study sites. Red lines indicate sub-catchment boundaries delineated by topography. (b) Schematic of benthic chamber used to quantify benthic fluxes during the seasonal campaigns, and photograph of a set of four chambers being deployed on the West Avon (Greensand). (c) Schematic and photograph of floating chamber used to quantify CO_2 and CH_4 outgassing during the seasonal campaigns including the underside of the chamber, showing the CO_2 sensor and battery pack, and a typical deployment (River Nadder on the Greensand). (d) Schematic of the automated floating chamber setup used to quantify CO_2 and CH_4 outgassing during the spring 2015 high-resolution campaign and the system deployed on the River Ebble on the Chalk. (e) Schematic representation of the aquatic eddy covariance technique and underwater photograph of a typical deployment (River Wylye on the Chalk).

Figure 2. Carbon gas sources and outgassing to the atmosphere. (a) average CO_2 outgassing rates across all six streams (n = 55), for each season in comparison to net-ecosystem-metabolism for either the benthic (NBM, n = 21) or whole stream (NWM, n = 21) metabolism. Note that positive NBM and NWM values indicate a source of CO_2. (b) CO_2 outgassing as a function of stream discharge normalized to sub-catchment area (n = 44). (c) average CH_4 outgassing rates (n = 16) in comparison to benthic release (n = 30) and (d) as for (b), but for CH_4 outgassing and discharge (n = 15). Box-plots (a, c) show the median (horizontal line), 25th and 75th percentiles and overall minimum and maximum values for each season across all six streams. Note that CH_4 outgassing rates and sediment release were not determined (n.d.) in spring. Scatter-plots in (b), and (d), give the partial residuals after fitting the individual outgassing rates for each stream, in each season as a function of discharge on each occasion (see Methods and Supplementary Information). (e) comparison between porewater CH_4 and CO_2 in piezometers in either streambed (n = 228) or adjacent riparian soils (n = 109) from Heppell & Binley (2016a). Values indicate the median. Chamber data are available from Rovelli et al. (2021b).

Figure 3. Sediment methane sources. *In situ* rates of CH_4 release from streambeds were greater in the dark (n = 140) than in the light (n = 141) and were also significantly different between the dominant streambed patch-types (gravel, sand, vegetated. n = 39, 72, 55, respectively). Note that the different patch-types were only a characteristic of the sand and Chalk-gravel streambeds and were not measured in the clay (n = 107). See Figures S4 and S8 and Table S3 for statistical analysis.

Figure 4 Contrasting diel changes in CO_2 and CH_4 outgassing. Outgassing of CO_2 was 27% greater at night than during the day (a), but consistent throughout for CH_4 (b). Each point in (a) and (b) is the average rate (in mmol m^{-2} h^{-1} ± s. e.) derived from three to four days of continuous measurements in each of the six streams in spring, 2015, with typically 230 flux estimates for each stream (see Figure S3; Rovelli et al. (2021a)). The black lines in (a) and (b), give the overall gradient and the grey line a 1:1 relationship. Note that the linear regressions were performed using the reciprocal of the standard error as weighting, to give robust average outgassing rates, with small standard errors more weight over those with larger standard errors. (c) the difference (Δ) between night and day outgassing rates for CO_2 (a) could partly be explained by reach-scale gross primary production (GPP_w, in mmol m^{-2} h^{-1}) in each stream (see Methods; Rovelli et al., 2017, 2018). (d) In contrast, the potential for biology to reduce CH_4 concentrations in the water column (methane oxidation on suspended

particulate matter, Rk_{CH4}) before being either outgassed (here as a reaeration constant, K_{CH4}) or diluted by the flow (K_{flow}) was negligible.

Figure 5 Simple reach-scale mass-balance modeling of diel changes in CO_2 and CH_4. (a) Changes in water column CO_2 and CH_4 are products of benthic uptake or release ($F_{streambed}$); activity in the water column ($F_{water\ column}$), e.g., oxidation for CH_4 and net ecosystem metabolism (NEM) for CO_2; outgassing at the stream surface ($F_{outgassing}$); transport from upstream (F_{in}); and advective transport downstream (F_{out}). (b) Example of development of new steady-state concentrations for CO_2 and CH_4 after the switch from day to night for the Chalk River Wylye. Background is the initial (t = 0) concentration in the water column ($C_{background}$), which is assumed equal to the concentration in water transported from upstream ($C_{upstream}$). (c) Modelled night outgassing rates *versus* observed mean outgassing rates during our high-resolution 2015 field campaign at the River Wylye (Chalk; green circles), Nadder (Greensand; blue squares) and Sem (clay; red triangles) for CO_2 (filled symbols) and CH_4 (open symbols). (d) The resultant change in rate of day to night outgassing, in percentage, for each gas based on (c).

1081 Figure 1

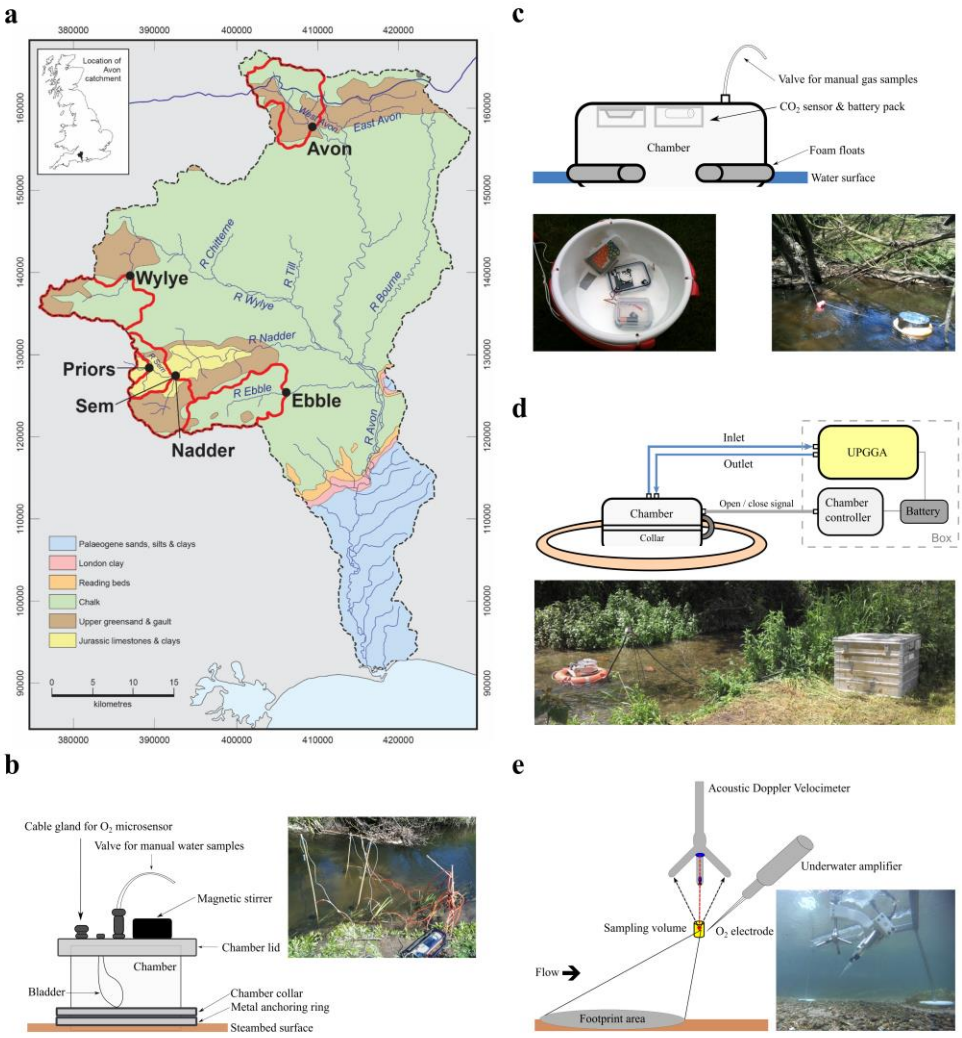

1082

1083 Figure 2

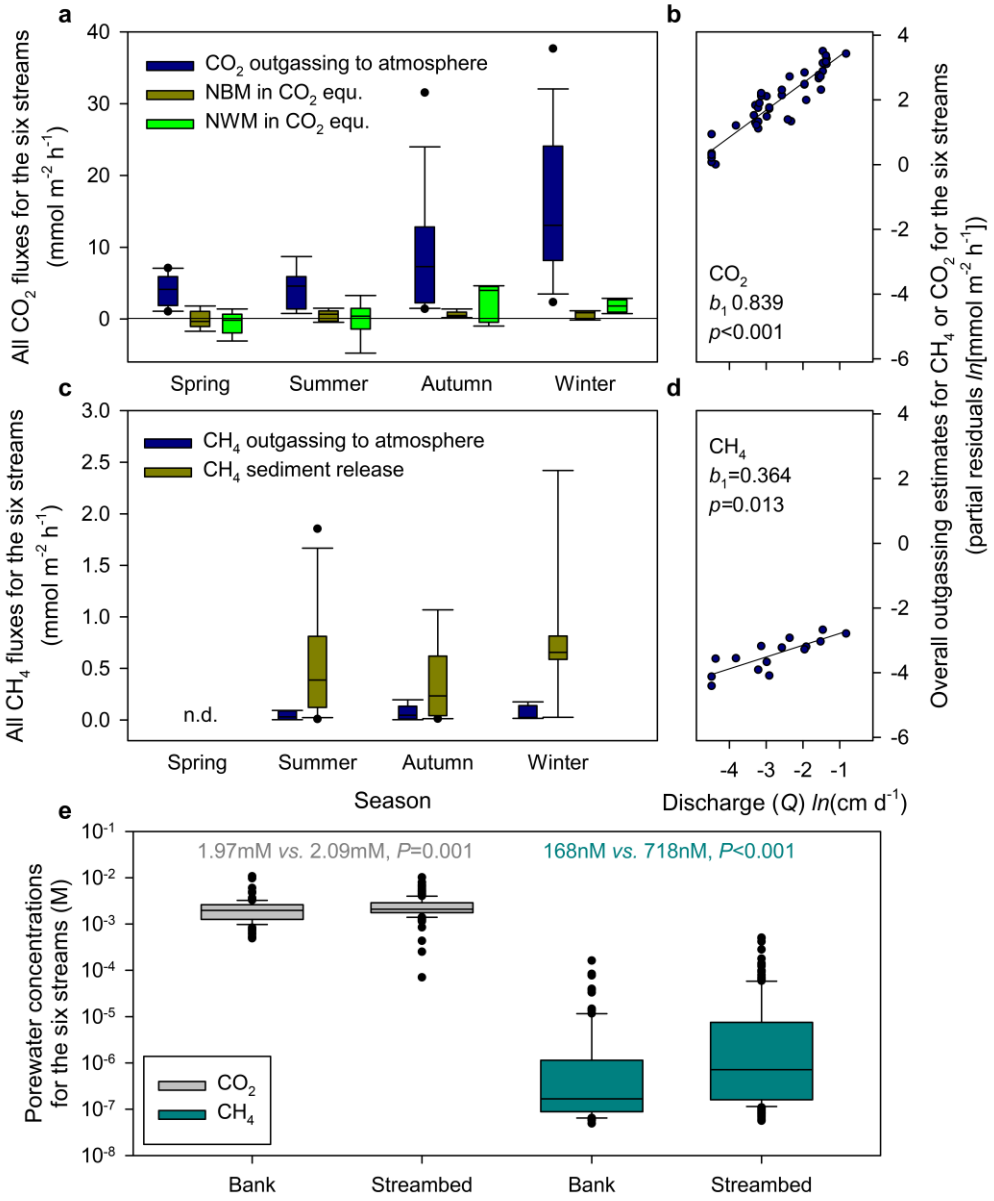

1084

1085 Figure 3

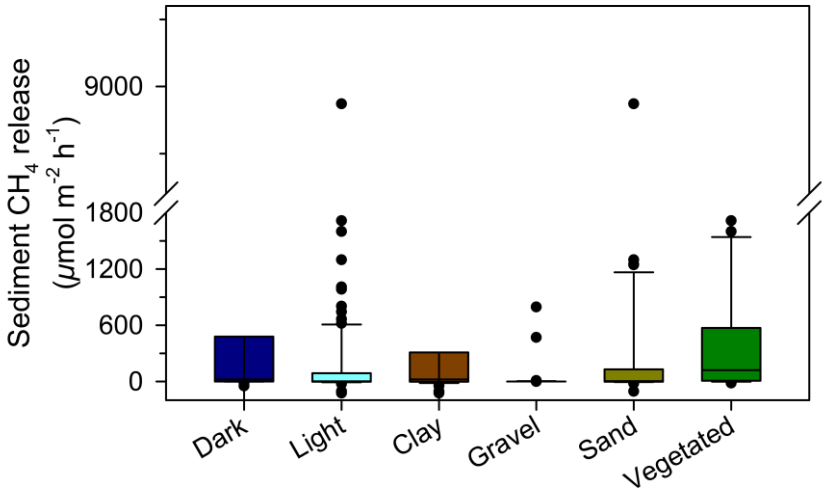

1086

1087 Figure 4

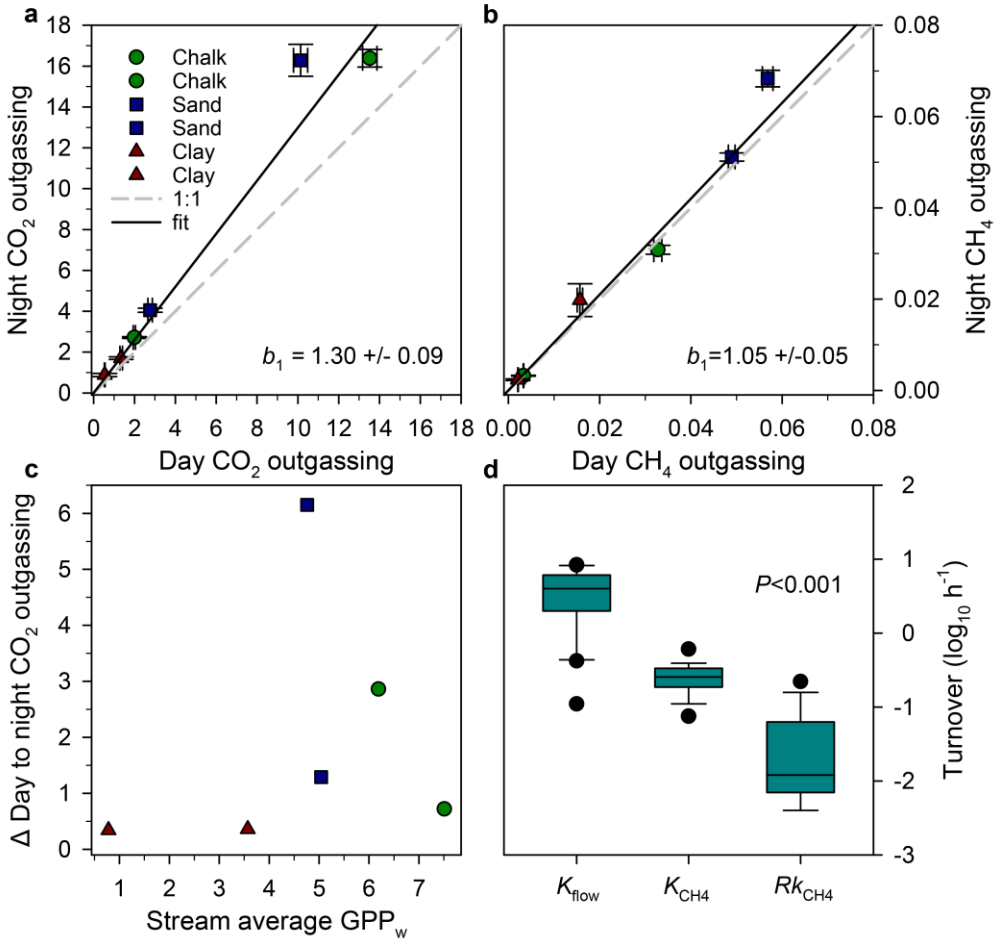

1088

1089 Figure 5

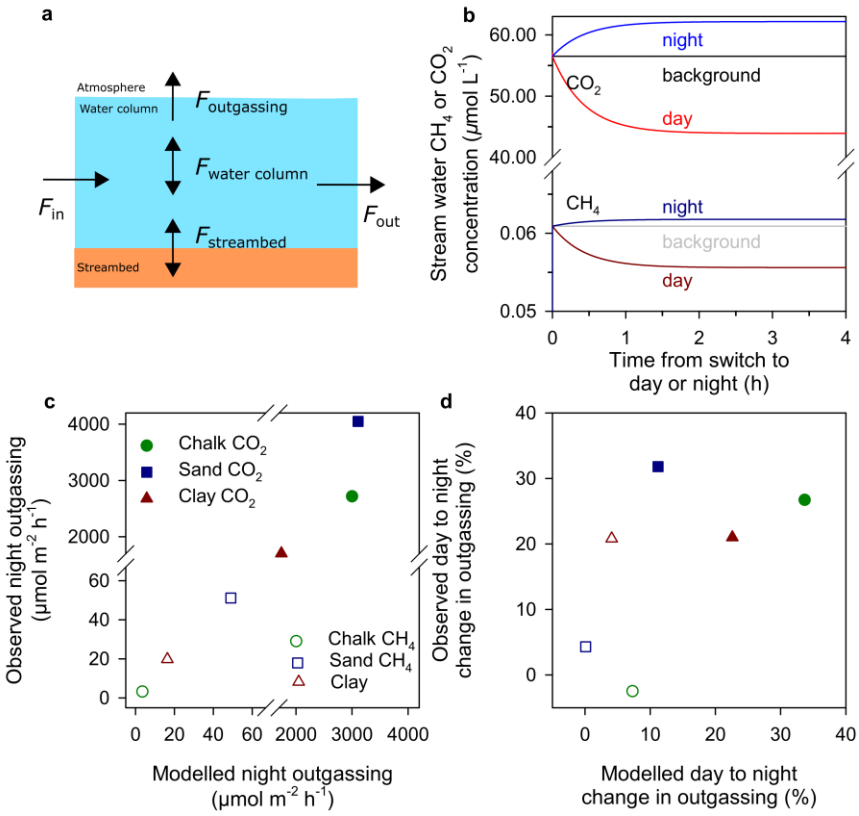

1090